

Structural and thermodynamic studies of n-butanol

This article has been downloaded from IOPscience. Please scroll down to see the full text article.

2010 J. Phys.: Condens. Matter 22 195102

(<http://iopscience.iop.org/0953-8984/22/19/195102>)

View [the table of contents for this issue](#), or go to the [journal homepage](#) for more

Download details:

IP Address: 129.252.86.83

The article was downloaded on 30/05/2010 at 08:05

Please note that [terms and conditions apply](#).

Structural and thermodynamic studies of n-butanol

I M Shmyt'ko¹, R J Jiménez-Riobóo², M Hassaine³ and M A Ramos³

¹ Institute of Solid State Physics of Russian Academy of Sciences, Chernogolovka, Moscow district, 142432, Russia

² Instituto de Ciencia de Materiales de Madrid, Consejo Superior de Investigaciones Científicas (ICMM-CSIC), Cantoblanco, E-28049 Madrid, Spain

³ Laboratorio de Bajas Temperaturas, Departamento de Física de la Materia Condensada, and Instituto de Ciencia de Materiales 'Nicolás Cabrera', Universidad Autónoma de Madrid, Cantoblanco, E-28049 Madrid, Spain

E-mail: miguel.ramos@uam.es

Received 10 February 2010, in final form 12 March 2010

Published 16 April 2010

Online at stacks.iop.org/JPhysCM/22/195102

Abstract

We have conducted x-ray diffraction, calorimetric and Brillouin-scattering experiments on n-butanol between 77 and 300 K, aiming to explore the physical nature of the so-called 'glacial state' previously found in n-butanol as well as in triphenyl phosphite. In addition to our structural and thermodynamic studies of the liquid–glass transition and of the stable crystal state in n-butanol, we have found that the metastable 'glacial state' that can be obtained in the temperature range 125–160 K is not a second amorphous state, but rather the result of a frustrated or aborted crystallization process that produces plenty of nanocrystallites embedded in a disordered matrix. The crystalline order of these nanocrystallites of the 'glacial phase' is exactly the same as that well observed in the fully ordered stable crystal into which it transforms by heating above 160 K.

(Some figures in this article are in colour only in the electronic version)

1. Introduction

The existence of *polyamorphic* [1, 2] transitions in molecular glass-forming liquids has been reported to occur in triphenyl phosphite (TPP) [3–9] and later also in n-butanol [10]. In both cases, a new solid phase denoted as *glacial phase* or *glacial state* [3, 4], obtained by a first-order, exothermic transformation from the supercooled liquid state was observed. For n-butanol, under isothermal conditions in the range 125–160 K, the supercooled liquid was found [10] to gradually transform into a white solid phase, which was identified as the same 'glacial state' reported for TPP. Although several experimental works have been published on TPP [2–9, 11–13] and, to a lesser extent, on n-butanol [8, 10, 14], the very nature of this allegedly new 'glacial state' remains controversial. Among others (see, for instance, [2]), the two most opposite reported views are to consider this unusual state: (i) as a manifestation of liquid–liquid transitions between two distinct liquid states (with their corresponding two distinct amorphous

states) even for a single-component substance [6–9]; (ii) as an aborted crystallization process due to a high crystal nucleation rate and a low crystal growth rate [11–14].

In a previous work, we have investigated [15] through calorimetric and elasto-acoustic Brillouin experiments the phase diagram of n-butanol and measured the specific heat and the thermal conductivity in a wide low temperature range for its three different states, namely glass, crystal and so-called 'glacial' states. Our experimental results showed that the obtained 'glacial state' in n-butanol was not an homogeneous, amorphous state, but rather a mixture of two different coexisting phases, very likely a collection of (frustrated) crystallites embedded in a disordered phase.

In the present work, we have extended this investigation by conducting x-ray diffraction experiments on n-butanol, so that the amorphous or crystalline character of this 'glacial state' could be properly addressed. Complementary new results obtained by calorimetry and Brillouin scattering will also be presented and jointly discussed. The concurrent use of these

three experimental techniques has already shown itself as very useful to unravel the puzzling phase diagram of other molecular glass-forming liquids such as ethanol [16].

2. Experimental details

2.1. Materials

High purity samples of n-butanol or 1-butanol (Aldrich, anhydrous grade, 99.8% pure, with nominal <0.005% water) were used without further purification.

2.2. X-ray diffraction

The molecular structure of liquid and solid states of n-butanol was investigated by means of x-ray diffraction experiments. An x-ray diffractometer D-500 (Siemens) with a secondary graphite monochromator and Cu K α radiation was used in transmission geometry. The liquid sample was inserted into a disk-like sample holder with beryllium disks of ~ 20 mm in diameter as windows. The thickness of the beryllium disks is ~ 0.1 mm and the distance between windows is ~ 1.0 mm. Besides the direct use of the beryllium disks as x-ray windows, they also served for adjusting the sample under investigation on the vertical axis of the x-ray goniometer. This was done in the following way: first of all, the x-ray detector is set in a position so that the diffraction angle corresponds to the (101) reflection of Be. Then, by shifting the cryostat with the sample holder along the direction of the incident beam, one gets the diffraction position of the output window of the sample holder and afterwards, by further moving the sample holder along the incident beam, the diffraction position for the input window is obtained. After this, the sample holder is positioned in the middle point between the so-determined beryllium window's positions. Because the angular spread of the incident beam was only 0.1° , it was possible to partially eliminate the reflections from the windows. The remnant parts of these beryllium reflections served as references. Because of the very small ($\sim 1.15 \times 10^{-5} \text{ K}^{-1}$) thermal expansion of Be, the sample holder was always adjusted in the position of (101) diffraction from beryllium at room temperature, it was not necessary to use additional adjustments of the equipment to get optimal scattering conditions for the sample.

The sample holder with n-butanol was inserted into a flow-type helium cryostat, designed and built in the Institute of Solid State Physics in Chernogolovka, Russia. This experimental set-up allowed us to vary the temperature and rate of cooling over a wide interval and provided a temperature control better than 0.1 K at a given constant temperature.

Two different measuring procedures were used. A first kind of procedure was used to conduct a detailed investigation of possible structural changes in n-butanol in a wide temperature interval. It consisted in a series of controlled temperature steps, where diffraction spectra were recorded, with the temperature decreasing from room temperature down to 96.8 K. The effective cooling rate of the sample in this case was very slow because the recording time of a single diffraction spectrum was approximately 2.5 h, that often was increased up to 15 h to improve statistics. A second procedure

was used to specifically obtain some crystalline or glassy phases of n-butanol. To obtain the stable crystal phase, slow cooling of the sample was performed from room temperature to a crystallization temperature T_{crystal} a few degrees below the melting point T_m . In order to obtain the glassy state, the sample was heated a few tens of degrees above T_m and then was quenched below the glass transition $T_g \approx 111$ K (in our case, into liquid nitrogen). After this, the quenched glass was slowly heated to several measuring temperatures, and also annealed at different temperatures for a few hours to observe and investigate crystallization processes.

2.3. Calorimetry and specific heat

Both calorimetric studies of the phase diagram of n-butanol and specific-heat measurements in the temperature range 80–220 K, were conducted by employing a versatile low temperature calorimetric system, especially designed for glass-forming liquids, which is described in more detail elsewhere [17]. On the one hand, this calorimetric system allows us to obtain thermograms by a direct display of the measured dT/dt curves as a function of temperature T , either for heating at a constant applied power or for certain annealing or cooling runs. On the other hand, accurate specific-heat values can also be obtained at the same time. Although our experimental method somewhat resembles commercial differential scanning calorimetry (DSC), it, however, allows direct measurements of the heat capacity based upon simple physical equations [17], without any ad hoc calibrations. A disadvantageous consequence of these relatively large ratios of sample/addenda masses needing to have accurate absolute data is that self-heating effects after big exothermic processes are unavoidable.

In this work, 463 mg of n-butanol were introduced into a copper calorimetric cell (of mass 1.293 g), which was immediately sealed to avoid contact with air moisture as much as possible. As previously described in more detail [16, 17], an electrical heater (1 k Ω) is glued onto the upper flat surface of the copper cell and a carbon ceramic sensor, attached to the lower surface of the calorimetric cell, is employed as thermometer. Experiments were run within a glass cryostat, with the calorimetric set-up inserted in a high-vacuum chamber ($\sim 10^{-7}$ mbar).

2.4. Brillouin spectroscopy

High-resolution Brillouin-scattering experiments in the temperature range 77–300 K were conducted by using an Ar⁺ ion laser (wavelength = 514.5 nm) and a Sandercock-type 3 + 3 tandem Fabry-Pérot interferometer. The experimental set-up was the same previously used [16, 18] for other glass-forming liquids such as ethanol.

A volume of 0.4 ml of n-butanol was extracted using a virgin syringe from the bottle and was rapidly introduced into a rectangular cuvette with transparent windows ($11 \times 41 \text{ mm}^2$) and an optical path of 1 mm (21/g/1 Starna[®]); the n-butanol sample occupied the whole cuvette so that no air was left inside. The cuvette was closed using the Teflon stopper provided and placed inside an optical cryostat. In order to

control the quality of the n-butanol sample, the refractive index of the liquid was determined by using a standard Abbe refractometer (Krüss) obtaining $n_{22.8^\circ\text{C}}^D = 1.3980 \pm 0.0001$. This value agrees very well with the refractive index reported⁴ for pure and dry n-butanol: $n^D(T_0) = 1.407424 - 4.1628 \times 10^{-4}T_0$, where T_0 is the temperature in Celsius. Since the refractive index of monoalcohols is very sensitive to small amounts of water [19], it is often used as a sensor to measure water content in alcohol. Our measurement confirms therefore that the liquid sample of n-butanol introduced in the cuvette did not contain a significant amount of water moisture or impurities. Low temperatures were achieved by using liquid nitrogen. An ITC-4 temperature controller (Oxford Instruments) was used in the experiments, obtaining a temperature stability of ± 0.05 K.

The optical cryostat (Optistat CF, from Oxford Instruments) is circular and is divided into an inner chamber and an outer chamber that vacuum isolates the inner one from the room temperature environment. A radiation shield can also be placed between both chambers for very low temperature requirements. The chambers are provided with four optical windows of $\varnothing 42$ mm for the outer ones and $\varnothing 15$ mm for the inner ones. The four windows are placed crossed at 90° and the inner and outer ones are coincident. In this way the performance of optical spectroscopy experiments is guaranteed, and also *in situ* taking of pictures is possible. The photographs were taken manually using an Olympus CAMEDIA C-7070 with a super macro. No flashlight was employed.

3. Results

3.1. Liquid and glass states

Figure 1 shows the temperature evolution of x-ray diffraction spectra of pure n-butanol, obtained in the liquid state at room temperature, at a few degrees above the melting temperature $T_m = 183.5 \pm 0.5$ K, and in the glass state by quenching the liquid sample from room temperature into liquid nitrogen. All these x-ray spectra are observed to consist of two halo-like reflections. As expected, on decreasing temperature the halfwidths of the two diffraction peaks get narrower and their centres of gravity are shifted to larger angles, corresponding to shorter intermolecular distances. Taking into account the 'ellipsoidal' shape of n-butanol molecules, we can interpret that the first peak at low diffraction angles reflects the typical intermolecular distance d_1 along the long axis of the molecule, whereas the second, main peak reflects the average short-axis distance d_2 between nearest-neighbour molecules, as depicted in figure 2.

The temperature variation of both long-axis (d_1) and short-axis (d_2) intermolecular distances, obtained from x-ray diffraction spectra such as those shown in figure 1, is presented in figure 3(a). From the slopes of the fitting linear curves for data in the liquid state, one can make an estimation of the thermal expansion coefficient of the liquid. Assuming that one third of the volume thermal expansion β is due to $d_1(T)$

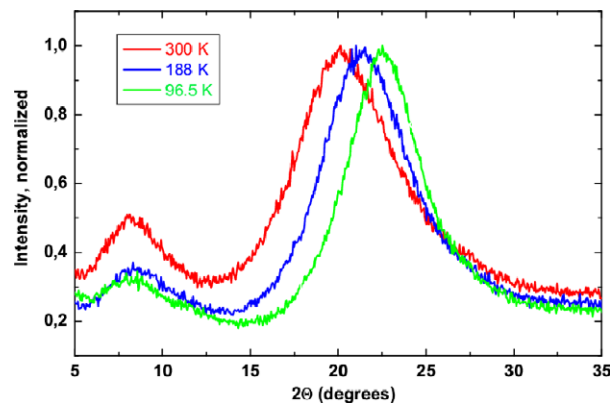


Figure 1. X-ray diffraction spectra of n-butanol, in the liquid state at 300 and 188 K, and in the glass state at 96.5 K, respectively from top to bottom.

variation and two thirds due to $d_2(T)$ variation, we obtain $\beta = (1.07 \pm 0.22) \times 10^{-3} \text{ K}^{-1}$, in good agreement with its value at room temperature $\beta = 0.948 \times 10^{-3} \text{ K}^{-1}$ [20]. In figure 3(b), we plot the corresponding temperature dependence of the halfwidth of the diffraction peaks, expressed in degrees, obtained for the first (d_1) and for the second (d_2) diffraction haloes.

As described in a previous work [15], n-butanol is a relatively good glass-former, and supercooling the liquid at a few K min^{-1} is more than enough to get the glass state. The measured molar specific heat of the so-obtained glass is shown in figure 4, together with the reference of those of the stable crystal and of the liquid above the melting temperature T_m . The glass transition is observed to occur at $T_g = 111 \pm 1$ K (when measured at a heating rate around $1\text{--}2 \text{ K min}^{-1}$), with a discontinuity of the specific heat of $\Delta C_p(T_g) = 48 \pm 2 \text{ J mol}^{-1} \text{ K}^{-1}$ between the baselines of the glass and liquid states. The specific heat of the supercooled liquid could not be measured above 120 K due to crystallization processes, as explained below.

3.2. (Stable) crystal state

In order to have a reliable reference for the above-mentioned discussions on possible intermediate or metastable phases, the fully ordered crystalline state should be studied first. The best way to obtain the stable crystal state of n-butanol is to anneal the supercooled liquid just below the melting temperature for a long time. In this situation, a good crystalline phase is formed, as can be seen in figure 5, after slowly cooling the liquid from 188 K and further annealing for 14 h at 179 K. The obtained x-ray diffraction pattern for this crystal at 179 K is obviously completely different to that of the liquid or glass states, and is typical of a low-symmetry crystalline order.

This crystalline structure was analysed with the aim of determining its crystal symmetry. For this purpose, the software POWD [21] was used. Four types of lattices were simulated: hexagonal, tetragonal, monoclinic and triclinic. The best definition for the F factor was obtained for the triclinic symmetry. The parameters resulting from the simulation were: primitive, $F27 = 7.5(.041, 87)$, $a =$

⁴ See Technical leaflet n-Butanol, BASF, March 2008.

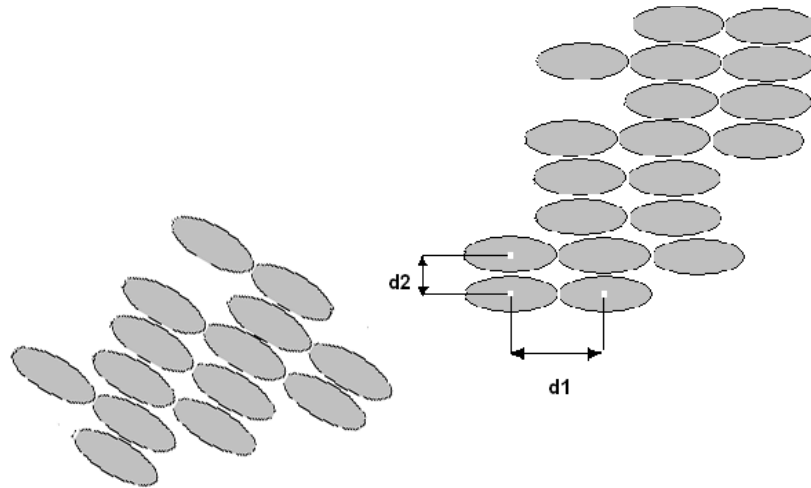


Figure 2. Schematic picture of the intermolecular packing of the nearest molecules along the long-axis direction of the molecules (d_1), and along the short-axis distance between them (d_2).

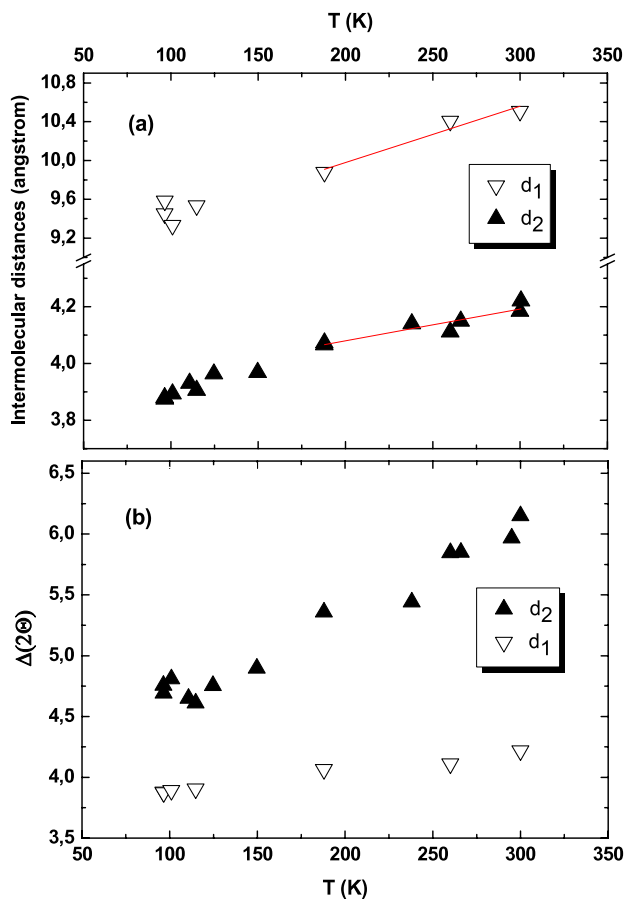


Figure 3. (a) Temperature dependence of average intermolecular distances in n-butanol obtained from the first (d_1) and from the second (d_2) diffraction peaks. Solid lines indicate linear fits to data points in the liquid state. (b) Temperature dependence of the halfwidth of the corresponding diffraction peaks, determined in degrees.

$5.439(5) \text{ \AA}$, $b = 9.458(7) \text{ \AA}$, $c = 8.05(1) \text{ \AA}$, $\alpha = 113.28(6)^\circ$, $\beta = 95.52(6)^\circ$, $\gamma = 96.49(1)^\circ$, $V = 373.5(1) \text{ \AA}^3$, with $N = 4$ molecules per unit cell. The calculation details are shown in table 1. As can be seen, the coincidence of the calculated

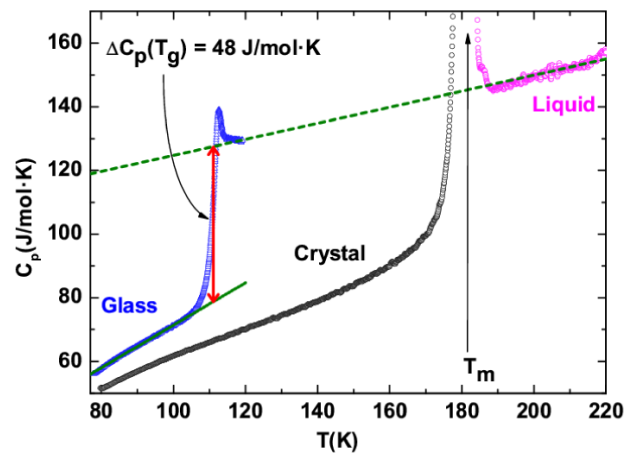


Figure 4. Specific heat of the glass state of n-butanol around the glass transition at $T_g = 111 \text{ K}$, where its specific-heat discontinuity is marked by an arrow, and of the stable crystal state up to the melting transition at $T_m = 183.5 \text{ K}$ into the liquid state.

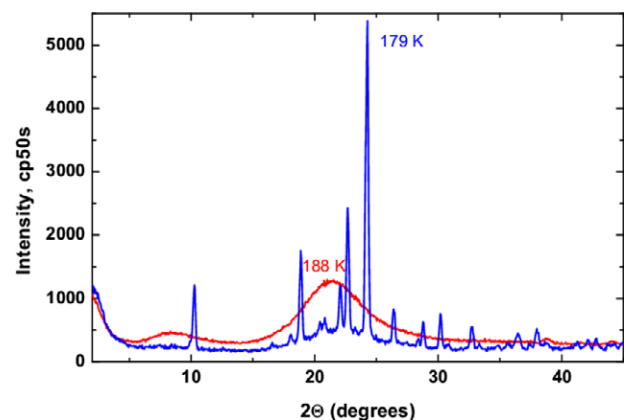


Figure 5. X-ray diffraction spectra of n-butanol, taken in the liquid state at 188 K, and in the crystal state at 179 K after cooling and annealing the former for 14 h.

reflection positions and the measured ones is not very good. However, we believe that the solution is still correct because only for this solution the reflections emerging at the first steps

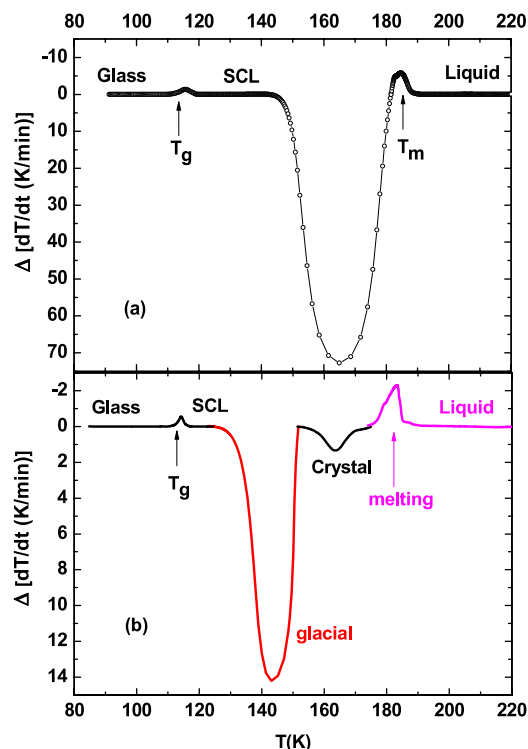


Figure 6. Thermograms as a function of temperature from the glass to the liquid, after subtraction of heat-capacity baselines of: (a) a continuous heating run at a constant applied power of 145 mW, which corresponds to a heating rate around 7 K min^{-1} of the SCL prior to crystallization, exhibiting a single crystallization process; (b) a slower heating run (around 1 K min^{-1}), followed by stabilization at 127 K, and continuation of the heating run after the ‘glaciation’ process has finished, featuring a smaller second crystallization peak and the endothermic melting process.

of crystallization (see figure 10) coincide with the cell axes directions. Let us mention that also high-pressure methanol (γ phase) [22] and 2-propanol [23] have been found to exhibit triclinic symmetry.

3.3. (Metastable) so-called ‘glacial state’

As shown and discussed in [15], when we heat the glass of n-butanol above its T_g , the supercooled liquid (SCL) undergoes an exothermic process (a first-order transition) into a so-called ‘glacial state’ above 125 K. Once this ‘glacial state’ has been obtained, it remains metastable, and when further heated above 155 K, it exhibits another exothermic, first-order transition into the stable crystal (see, for instance, figure 1 of [15]). We have also been able to obtain this metastable ‘glacial state’ of n-butanol by directly cooling the liquid down to a stabilization temperature within the temperature range 125–145 K, approximately (see figure 2 of [15]).

In figures 6 and 7, we present new thermograms to illustrate our observations on the phase diagram of n-butanol. In all of them, we have subtracted the heat-capacity baselines (measured in our calorimetric system in terms of dT/dt), so that endothermic and exothermic processes corresponding to the different phase transitions are emphasized. In figure 6, they are plotted as a function of temperature, whereas in figure 7 the

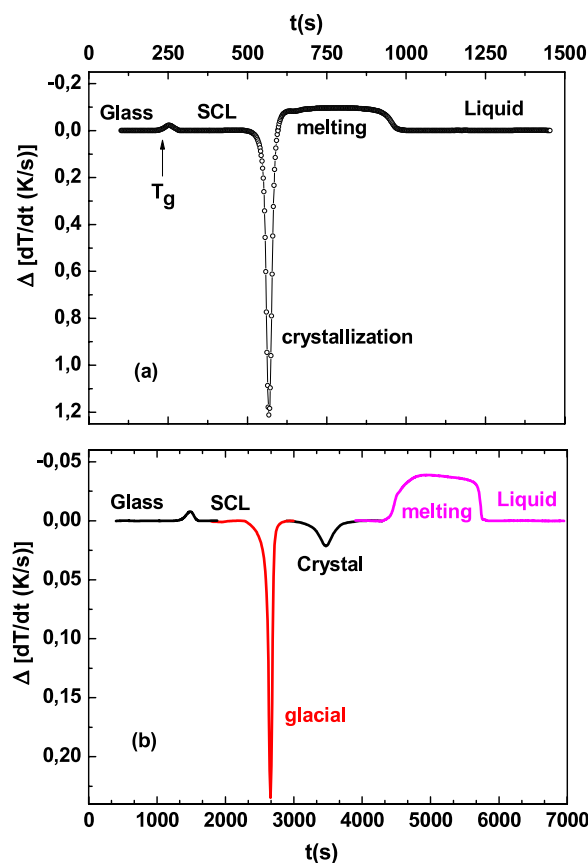


Figure 7. Same thermograms as figure 6 after subtraction of heat-capacity baselines, but as a function of time: (a) a continuous heating run applying 145 mW (corresponding to a heating rate around 7 K min^{-1} of the SCL prior to crystallization) exhibiting a single crystallization process; (b) a slower heating run (around 1 K min^{-1}), followed by stabilization at 127 K, and continuation of the heating run after the ‘glaciation’ process has finished, featuring a smaller second crystallization peak and the endothermic melting process.

same runs are plotted as a function of time, since they provide complementary information. Figures 6(a) and 7(a) show a continuous heating run at a constant applied power of 145 mW (corresponding to a heating rate around 7 K min^{-1} of the SCL prior to crystallization) that exhibits a single crystallization process above 146 K. Since such a relatively high applied power is not turned off here, and due to the appreciable self-heating effects mentioned above, the (single) crystallization process ends almost at the melting temperature. Figures 6(b) and 7(b) have been composed of several consecutive runs: a slower heating run at 25 mW (around 1 K min^{-1}) of the glass is followed by isothermal stabilization at 127 K. Once the observed exothermic ‘glaciation’ process has finished, the same power of 25 mW is again applied until a smaller, second crystallization step occurs. Finally, the endothermic melting process is produced by applying 64 mW.

We have also followed a similar procedure to investigate the structural properties of these phases via x-ray diffraction experiments. To start from the glass state, the liquid was quenched as follows. The sample holder was inserted into a column of the x-ray cryostat at room temperature and it was

Table 1. Details of POWD software calculations of the crystalline cell of n-butanol from the experimental positions of Bragg reflections: line ordering number, calculated and observed d -spacing, relative intensity of the peaks, Miller indices, observed and calculated scattering angle 2θ and their corresponding difference.

Line #	d -spacing (\AA)		Intensity	Indices			2θ , degree		Diff.
	obs.	Calc.		h	k	l	Obs.	Calc.	
1	8.5724	8.5681	22.0	0	1	0	10.32	10.32	-0.004
2	5.3317	5.3390	1.6	1	0	0	16.63	16.60	0.026
3	4.8980	4.9099	4.2	-1	1	0	18.11	18.07	0.044
4	4.6862	4.6902	29.0	0	1	1	18.94	18.92	0.020
5	4.3183	4.3187	4.0	-1	-1	1	20.57	20.57	0.005
6	4.2476	4.2640	3.9	1	-1	1	20.91	20.83	0.078
7	4.0150	4.0072	14.0	0	-1	2	22.14	22.18	-0.043
8	3.9087	3.9102	36.0	-1	1	1	22.75	22.74	0.009
9	3.6592	3.6543	100.0	0	0	2	24.32	24.36	-0.037
10	3.3649	3.3598	11.0	-1	-2	1	26.49	26.53	-0.039
11	3.1347	3.1316	3.0	0	-3	1	28.47	28.50	-0.031
12	2.9504	2.9522	7.2	0	1	2	30.29	30.27	0.016
13	2.8968	2.9015	1.2	0	-3	2	30.87	30.82	0.054
14	2.6789	2.6774	1.6	-2	1	0	33.45	33.47	-0.018
15	2.6051	2.5991	0.7	1	-3	2	34.42	34.51	-0.086
16	2.5685	2.5751	1.4	-1	-3	1	34.93	34.84	0.091
17	2.5145	2.5144	1.7	-2	-1	1	35.71	35.71	0.003
18	2.4575	2.4550	4.3	-2	2	0	36.56	36.60	-0.042
19	2.3963	2.3957	2.2	2	-2	1	37.53	37.54	-0.012
20	2.3621	2.3613	4.8	1	3	0	38.10	38.11	-0.009
21	2.2366	2.2340	1.0	-2	-2	1	40.32	40.37	-0.052
22	2.1877	2.1876	1.5	-2	1	2	41.27	41.27	0.002
23	2.1824	2.1826	1.5	1	-4	2	41.37	41.37	0.003
24	2.1398	2.1420	2.8	0	4	0	42.23	42.19	0.043
25	2.1094	2.1122	2.7	-1	4	0	42.87	42.81	0.059

closed to stop the flow of liquid nitrogen onto the holder. Then the column was rapidly opened, so that liquid nitrogen flew from the nitrogen chamber through a special capillary onto the holder. When the area around the holder was filled with liquid nitrogen, the temperature controller was turned on and the sample was heated up to the set-point temperature.

Figure 8 shows the evolution with temperature of x-ray diffraction spectra at slow heating, starting from the frozen liquid (i.e. the glassy state) at 96.5 K. The figure is split in two temperature regions: (a) the formation of the so-called 'glacial state'; (b) the second crystallization step from the previous 'glacial state' to the fully ordered crystalline state.

In figure 8(a), superimposed on the amorphous background (of the SCL) one can clearly see the emergence of crystalline peaks at 127 K, that becomes better defined at 130.2 K and is already completed at 134.8 K. It is to be noted that the growth of these crystalline reflections is, however, accompanied by keeping a big part of the amorphous background. As shown in figure 8(b), subsequent heating of the sample up to 155 K does not produce any further structural changes. Above 155 K, the previously formed 'glacial phase' begins to transform into the fully ordered crystalline phase of n-butanol that is undoubtedly observed at 180 K. Let us remark that the emergent crystalline peaks at 127 K in the 'glacial phase' are exactly the main Bragg peaks of the stable crystal phase. Furthermore, this crystal phase obtained after heating from the 'glacial' one and the crystal phase prepared by slowly

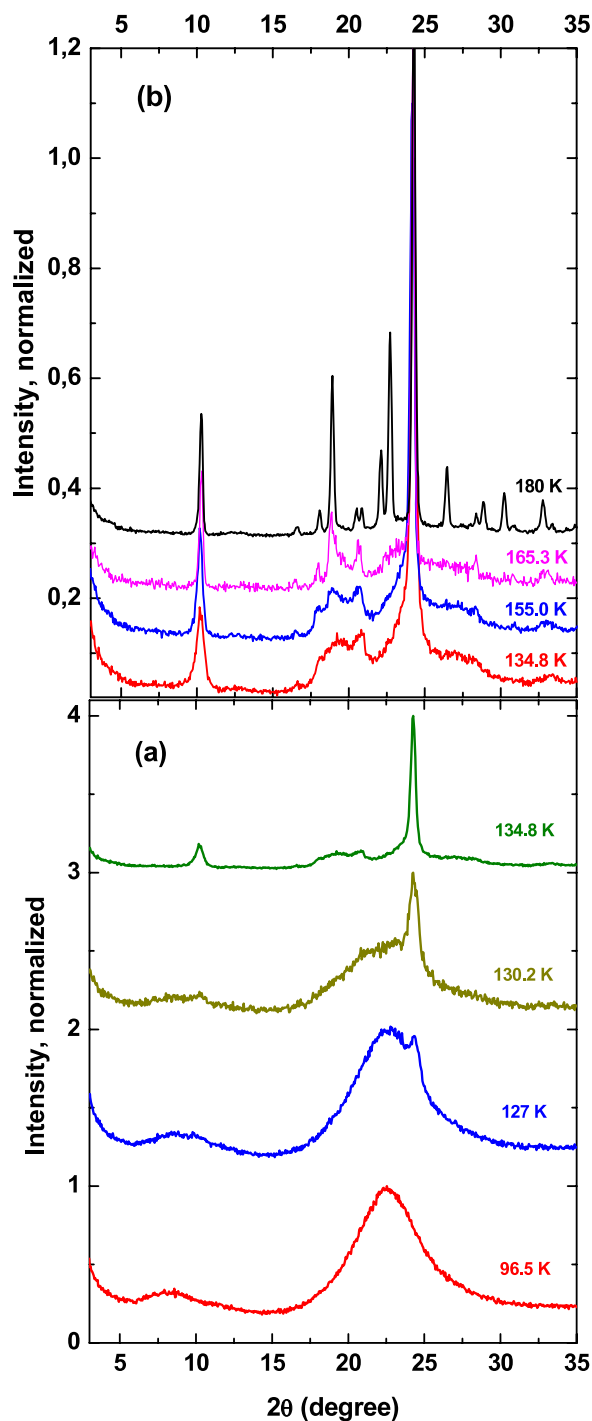


Figure 8. Evolution with temperature of x-ray diffraction spectra at slow heating, starting from the glassy state: (a) emergence of crystalline peaks superimposed on the amorphous pattern for the so-called 'glacial phase' at 127 K; (b) full crystallization of n-butanol above 155 K. All spectra have been shifted vertically for clarity.

cooling the liquid to 179 K (see figure 5) are exactly the same and stable, as a direct comparison shows in figure 9.

We present in figure 10 the x-ray diffraction spectrum obtained after cooling the liquid to 140 K, also showing as a reference the spectrum of the liquid at 188 K. Although plotted in a different scale, the diffraction pattern is almost identical to that obtained for the 'glacial phase' at 134.8 K (figure 8)

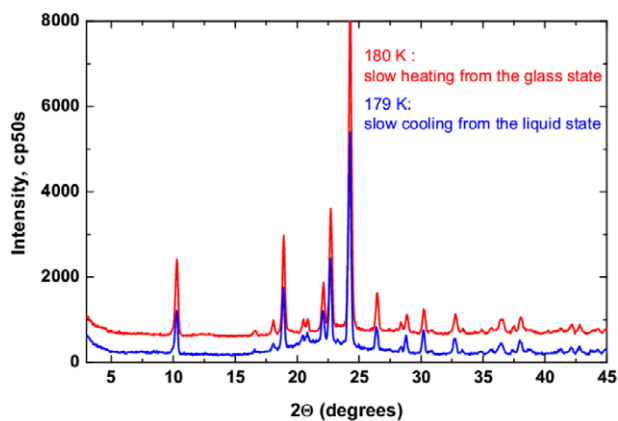


Figure 9. Comparison of x-ray diffraction spectra of the crystal obtained after a slow heating run starting from the glass state up to 180 K (above) and that obtained after slow cooling from the liquid state and stabilization at 179 K (below).

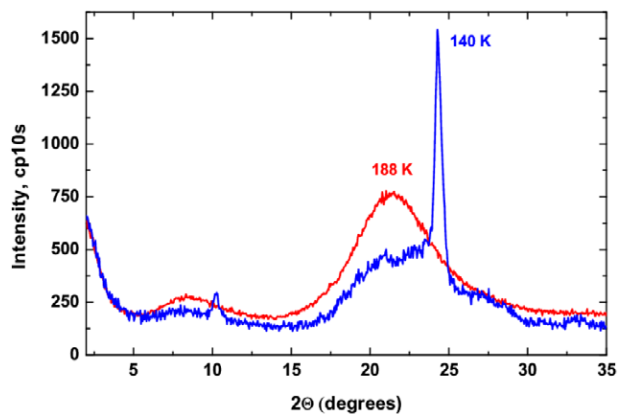


Figure 10. X-ray diffraction spectrum obtained after cooling the liquid to 140 K, using a recording time of about 2.5 h. As a reference, an x-ray diffraction spectrum of the liquid at 188 K (using a recording time of about 15 h) is also shown.

by heating the SCL. This is in agreement with our earlier observations by calorimetry (see figures 1 and 2 of [15]). It can be clearly seen in figure 10 that the first steps of the ‘glacial’ crystallization are characterized by the emergence of only two narrow (crystalline-like) reflections meanwhile conserving most of the two-haloes amorphous-like spectrum characteristic of the supercooled liquid. Such a structural state can indeed be described as the first step of the crystallization process. The growing nanocrystallites exhibit tetragonal symmetry of the lattice cell, since only two reflections are expressed well. The crystalline structure of the unit cell might be more complex (for example, it could be monoclinic), but the absence of high-quality pronounced reflections of weak intensity has led us to conclude that the quality of molecular ordering in the growing nanocrystallites cannot be very high in any case.

Brillouin-scattering experiments [15] confirm the above-mentioned view about the mixed-nanocrystalline nature of the ‘glacial phase’ in n-butanol. The upper panel of figure 11 shows the temperature evolution of the backscattering Brillouin-frequency shifts $f^{180}(T)$ either on heating the

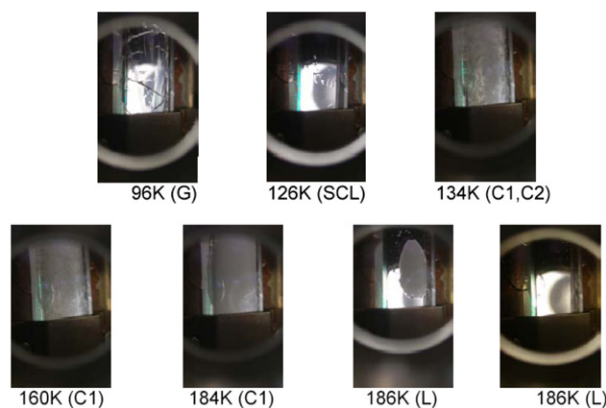
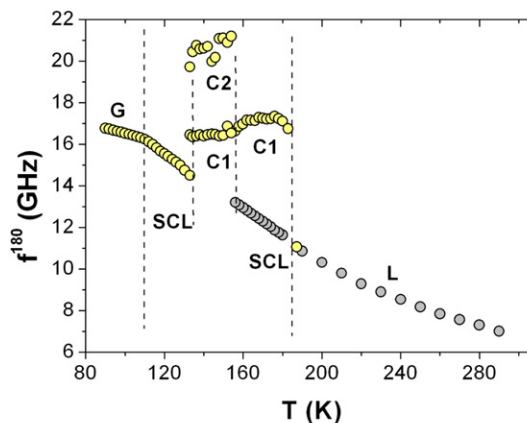


Figure 11. Top: temperature evolution of the backscattering Brillouin-frequency shifts $f^{180}(T)$ on heating after quenching from room temperature (RT) to 90 K (light circles) and on slowly cooling from RT (dark circles). G: glass phase; SCL: supercooled liquid; C1 and C2: ‘glacial’ and crystalline phases; L: liquid. Bottom: optical photographs at different temperatures showing the different aspects of the sample throughout the different phases. The sample is found inside the cryostat. The round bright features in the photographs correspond to the frame of the inner window of the cryostat and are brighter when the sample is transparent and the light from the laboratory can come through.

glass (light circles) or on slowly cooling the liquid from room temperature (dark circles). Starting from the lowest temperatures, the glass transition is observed at about 110 K. Then, the structural transition from the viscous supercooled liquid into a crystalline-like state (the so-called ‘glacial’ state) occurs at about 132 K, where two phonon peaks (C1 and C2) are seen to coexist, supporting the statement that the ‘glacial state’ corresponds to a mixture of two different phases. Above 156 K, the substance is able to fully crystallize, and only the truly crystalline phonon peak (C1) remains [15] until the melting point at 184 K.

4. Discussion

As can be seen in figure 1, the first x-ray diffraction peak is much weaker than the second one, in contrast to what is typically observed in amorphous metals and semiconductors. This behaviour is, however, the same previously observed in other similar glass-forming monoalcohols such as ethanol [16]

or propanol [24]. It can be attributed to the 'ellipsoidal' shape of these monoalcohol molecules that tends to favour a local arrangement of molecules along the short-axis direction (d_2) compared to that along the long axis (d_1).

It is also worthwhile paying attention to the redistribution of the intensities of these two diffraction peaks as a function of temperature. Since the intensities essentially reflect the number of neighbours, the decreasing of the intensity of the first halo with decreasing temperature means that the number of the nearest-neighbour *contacts* (see figure 2) of pairs of butanol molecules along the *long axis* decreases with decreasing temperature. This can be interpreted as the coherent reflection volumes (the collection of molecules which produce this x-ray diffraction reflection) changing from spherical ones at high temperature to columnar or disk-like ones at lower temperatures.

As it is well known, for crystals the reflection positions found in the diffraction experiments are defined by the Bragg equation: $2d \sin \theta = \lambda$, where λ is the x-ray wavelength, θ is the diffraction angle and d is the interplanar spacing. For liquid and amorphous states the position of the first halo could be defined by an analogous equation [25]: $2R_1 \sin \theta = 1.23\lambda$, where R_1 stands for the shortest distance between neighbour atoms or molecules and 1.23 is a correction coefficient. In our case R_1 denotes the nearest distance between the centres of gravity of the butanol molecules. If there is some ordering between molecules the correction coefficient must be changed, but it always lies in the 1.1–1.2 interval. The exact value of this correction coefficient is difficult to calculate. For this reason, in figure 3(a) we have determined the intermolecular distance as an interplanar distance (i.e. the correction coefficient is equal to 1.0). Therefore the real intermolecular distances may be systematically some 10–20% larger than those shown, and this unknown pre-factor could be different for short and long axes of the ellipsoidal molecules.

In figure 3(b), the temperature dependence of the halfwidths of the two haloes is shown. If we assume that the halo-like spectrum reflects the stochastic distribution of the butanol molecules (i.e. an ideal amorphous state), then the halfwidth defines the degree of local disorder in the molecule distribution. In principle, it has not to change with temperature. The observed narrowing of the width of the haloes implies that the coherent length of the x-ray scattering increases with decreasing temperature. In other words, the ordering of the molecules improves with decreasing temperature, both for short (second halo) and long (first halo) intermolecular distances.

We can use the halfwidth of the diffraction reflections to quantify the mean size of the formed nanocrystallites in the 'glacial phase' and the mean size of the crystallites in the stable crystalline state. It is known that the halfwidth of the diffraction reflections is determined by the crystallite dimension $\langle D \rangle$, by the dispersion of the lattice parameters inside the crystallites $\delta d/d$, by the nonmonochromaticity of the radiation used $\delta\lambda/\lambda$ and by parameters of the experimental geometry. As a rule, for the correct determination of the crystallite dimensions it is needed to analyse a few orders of the reflections, which unfortunately is not possible in our

case. For this reason we can only estimate the mean size of the crystallites. If we assume that the halfwidth of the reflections is only defined by the mean size of the crystallites, we can calculate the lower limit of these dimensions. The least value of the mean size of nanocrystallites can be evaluated by using Scherrer's formula [25]: $\Delta(2\theta) = K\lambda/\langle D \rangle \cos \theta$, where θ is the diffraction angle, $K \sim 1.0747$ and $\langle D \rangle$ is the mean diameter of the area of coherent scattering. For the correct determination of the halfwidth of the reflections, the appropriate parameters of the equipment for the used transmission geometry were taken into account. The least value of the mean size of nanocrystallites in the 'glacial phase' was found to be 28 nm along the d_1 direction and 62 nm along the d_2 direction. They remain essentially constant in the temperature region 135–155 K, see figure 8(b). After full crystallization of the sample (by annealing at 180 K for 15 h) the least values of the mean size of crystallites along d_1 and d_2 directions increase significantly. The calculations give values which tend to infinity. Since in our experiments the so-called 'two-crystal geometry' was used, crystallite dimensions larger than 100 nm are unsolvable. Therefore, we can conclude that the mean size of the crystallites in the final fully ordered crystalline phase has achieved at least a micrometre range.

As indicated above, the glass transition of n-butanol occurs at $T_g = 111 \pm 1$ K, with a discontinuity of the specific heat of $\Delta C_p(T_g) = 48 \pm 2$ J mol⁻¹ K⁻¹. In comparison with published values [26] of the smaller members of the series (methanol, ethanol and n-propanol), it is noteworthy that T_g is clearly higher (in the three former cases, $T_g \approx 95$ –100 K) whereas $\Delta C_p(T_g)$ increases monotonically with the number of carbons (30, 38 and 45 J mol⁻¹ K⁻¹ for methanol, ethanol and n-propanol, respectively). A similar behaviour as that of $\Delta C_p(T_g)$ is found for the entropy of melting ΔS_m : for n-butanol we have $\Delta S_m = 50.5 \pm 0.5$ J mol⁻¹ K⁻¹, to be compared with ΔS_m of 22, 31 and 37 J mol⁻¹ K⁻¹ for methanol, ethanol and n-propanol, respectively.

The obtained photographs (see lower part of figure 11) clearly show the evolution of the sample on heating after quenching from room temperature to 90 K. At 90 K the sample is completely transparent, as expected for a sample in the glassy state, except for some macroscopic cracks arising from stresses between the n-butanol sample and the cuvette surface due to different thermal expansion coefficients. At 126 K the sample is in the supercooled liquid state after passing through the glass transition (exhibiting a kink-like anomaly in $f^{180}(T)$, as shown in the upper part of figure 11). In this case the sample is completely transparent and no cracks are visible, as expected for a liquid. When the sample goes above 130 K, entering the so-called 'glacial phase', something changes dramatically. The picture taken at 134 K clearly shows this. The sample is no longer transparent, which is in clear contradiction to a typical liquid or glass, since both of them are isotropic. If there was a liquid state, it should be only a part of the whole, because opacity is a clear sign either of micro-cracks, which could hardly be understood in a liquid, or of the existence of microcrystalline structures embedded in a liquid matrix, or of the existence of a unique non-cubic polycrystalline phase. At higher temperatures (see the photograph at 160 K) the picture

does not change significantly, even though the existence at about 156 K of a phase transition from the so-called 'glacial' phase to the crystalline stable phase is well established. At 184 K the sample seems to be more homogeneous just before the beginning of the melting process, that is clearly visible in the photographs taken at 186 K at two different times. This series of photographs confirms, therefore, that the metastable 'glacial' state does not correspond to a second isotropic liquid-glass state, but it is rather some kind of disordered, not well-grown crystal.

5. Conclusion

Our x-ray diffraction experiments on n-butanol, together with earlier and new calorimetric and Brillouin-scattering ones, support the conclusion that the so-called 'glacial phase' is not a second amorphous state, but rather the result of a frustrated crystallization process that produces many nanocrystallites embedded in a more or less disordered matrix. This is evidenced by the emergence of the crystalline Bragg peaks onto the amorphous diffraction pattern. We have estimated that the size of these nanocrystallites is of several tens of nanometre. Then, by further heating this intermediate, metastable phase, the fully crystallized state is obtained: the diffraction pattern exhibits a fully crystalline pattern (ascribed to a triclinic symmetry), but with crystallite size in the micrometre range rather than in the nanometric one as in the 'glacial' phase. The same crystalline phase is obtained by slowly cooling or isothermal crystallization of the liquid at high enough temperatures. Hence the concept of *polyamorphism* does not apply to the case of n-butanol, at least.

On the other hand, glass and crystal states exhibit similar structural and thermodynamic properties to those of propanol. Interestingly, from a quantitative point of view, n-butanol values are closer to those of *iso*-propanol rather than to those of *n*-propanol, especially concerning the T_g values for their glass states [23] or the unit-cell parameters for their crystal states [24], though the latter should always be used with caution.

Acknowledgments

This work was financially supported in part by the Spanish Ministry of Science within project FIS2009-09811 and program CONSOLIDER Nanociencia Molecular CSD2007-00010, as well as by the Comunidad de Madrid through program 'Science and Technology in the Millikelvin' (S-0505/ESP/0337).

References

- [1] Angell C A 1995 *Science* **267** 1924
- [2] Senker J and Rössler E 2001 *Chem. Geol.* **174** 143
- [3] Ha A, Cohen I, Zhao X, Lee M and Kivelson D 1996 *J. Phys. Chem.* **100** 1
- [4] Cohen I, Ha A, Zhao X, Lee M, Fischer T, Strouse M J and Kivelson D 1996 *J. Phys. Chem.* **100** 8518
- [5] Wiedersich J, Kudlik A, Gottwald J, Benini G, Roggatz I and Rössler E 1997 *J. Phys. Chem. B* **101** 5800
- [6] Tanaka H, Kurita R and Mataka H 2004 *Phys. Rev. Lett.* **92** 025701
- [7] Kurita R and Tanaka H 2004 *Science* **306** 845
- [8] Kurita R and Tanaka H 2005 *J. Phys.: Condens. Matter* **17** L293
- [9] Kurita R, Shinohara Y, Amemiya Y and Tanaka H 2007 *J. Phys.: Condens. Matter* **19** 152101
- [10] Bol'shakov B V and Dzhonson A G 2003 *Dokl. Phys. Chem.* **393** 318
Bol'shakov B V and Dzhonson A G 2005 *J. Non-Cryst. Solids* **351** 444
- [11] Hédoux A, Guinet Y and Descamps M 1998 *Phys. Rev. B* **58** 31
- [12] Hédoux A, Hernandez O, Lefèbvre J, Guinet Y and Descamps M 1999 *Phys. Rev. B* **60** 9390
- [13] Hédoux A, Guinet Y, Foulon M and Descamps M 2002 *J. Chem. Phys.* **116** 9374
- [14] Wypych A, Guinet Y and Hédoux A 2007 *Phys. Rev. B* **76** 144202
- [15] Hassaine M, Jiménez-Riobóo R J, Sharapova I V, Korolyuk O A, Krivchikov A I and Ramos M A 2009 *J. Chem. Phys.* **131** 174508
- [16] Ramos M A, Shmyt'ko I M, Arnautova E A, Jiménez-Riobóo R J, Rodríguez-Mora V, Vieira S and Capitán M J 2006 *J. Non-Cryst. Solids* **352** 4769
- [17] Pérez-Enciso E and Ramos M A 2007 *Termochim. Acta* **461** 50
- [18] Jiménez-Riobóo R J, Kabtoul B and Ramos M A 2009 *Eur. Phys. J. B* **71** 41
- [19] Jiménez-Riobóo R J, Philipp M, Ramos M A and Krüger J K 2009 *Eur. Phys. J. E* **30** 19
- [20] Cerdeiriña C A, Tovar C A, González D, Carballo E and Romaní L 2001 *Fluid Phase Equilib.* **179** 101
- [21] Wu E 1989 *J. Appl. Crystallogr.* **22** 506
- [22] Allan D R, Clark S J, Brugmans M J P, Ackland G J and Vos W L 1998 *Phys. Rev. B* **58** R11809
- [23] Talón C, Bermejo F J, Cabrillo C, Cuello G J, González M A, Richardson J W Jr, Criado A, Ramos M A, Vieira S, Cumbreña F L and González L M 2002 *Phys. Rev. Lett.* **88** 115506
- [24] Talón C, Ramos M A, Vieira S, Shmyt'ko I, Afonikova N, Criado A, Madariaga G and Bermejo F J 2001 *J. Non-Cryst. Solids* **287** 226
- [25] Guinier A 1956 *Theorie et Technique de la Radiocristallographie* 2nd edn (Paris: DUNOD) p 604
- [26] Wang L M, Angell C A and Richert R 2006 *J. Chem. Phys.* **125** 074505